17

Potential for Improving HD Diesel Truck Engine Fuel Consumption Using Exhaust Heat Recovery Techniques

D.T. Hountalas[1] and G.C. Mavropoulos[2]
[1]*Professor of Internal Combustion Engines, Dipl.Ing., Dr.Ing. (NTUA)*
[2]*Research Associate, Internal Combustion Engines Dipl.Ing., Dr.Ing. (NTUA), M. SAE, M. ACS*
Internal Combustion Engines Laboratory
Thermal Engineering Department
School of Mechanical Engineering
National Technical University of Athens (NTUA)
9 Iroon Polytechniou St., Zografou Campus, 15780 Athens, Greece

1. Introduction

Increased fuel costs and diminishing petroleum supplies are forcing both governments and industries to reduce engine fuel consumption. Up to now significant improvement has been achieved towards this direction using advanced engine techniques such as downsizing, VVT, advance fuel injection, advanced boosting etc. However the potential for further significant improvement is extremely limited.

Despite these advancements diesel engines still reject a considerable amount of fuel chemical energy to the ambience through the exhaust gas. This is approximately 30-40% of the energy supplied by the fuel depending on engine load. If part of this thermal energy is recovered and converted to power it could result to a significant reduction of engine bsfc. To achieve this various techniques are available some of which have been partially tested in the past. Mechanical turbocompounding is considered a base technology which combines the output of a diesel engine with that of an exhaust gas driven turbine located downstream of the turbocharger turbine. Electrical turbocompounding is a similar technique using an efficient turbocharger turbine and a high speed generator mounted on the turbocharger's shaft. The excess turbine power is converted to electricity. However both techniques can be significantly improved especially using advanced turbocharging components and relevant techniques to control and vary power turbine pressure ratio or exhaust manifold pressure (electric turbocompounding) with operating conditions. Another promising technology is the use of a Rankine Bottoming Cycle with steam or organic as working media. Its use has special difficulties for truck applications due to size limitations, packaging and the negative impact on the engine primary cooling system. Therefore special care is necessary when studying such an application.

In the present is made an effort to evaluate the potential bsfc improvement of HD diesel engines using the aforementioned technologies for exhaust gas heat recovery. For this reason results from the analysis on a heavy duty truck diesel engine at various speeds and loads are presented. Results are based on simulation models developed and used to simulate the aforementioned configurations. Special attention is given to the identification of the potential efficiency gain and mainly to the various problems that have to be resolved for a vehicle application. As shown there exists a strong potential for the application of these techniques since a reduction of fuel consumption from 3% up to 12-13% depending on the technology is achievable.

In 2006, the emissions from transportation sources in the USA reached an amount of 40% of the total Greenhouse gas emissions in this country. Medium and heavy-duty vehicles represent about 22% of the transportation emissions. The use of trucks is energy-intensive and accounted for 69% of freight energy use, consuming 2.35 million barrels of oil per day in 2008 and generating 363 million metric toned of carbon dioxide. Hence trucks are one of the top priorities when looking for energy savings and climate change mitigation in the transportation sector.

2. The NTUA engine simulation model

During the last years, the high interest in the examination of potential benefits from the use of exhaust gas heat recovery systems, has motivated a number of companies and research institutes to develop models appropriate for the simulation of such energy systems.

An extensive evaluation of potential benefits concerning engine performance and bsfc improvement for the available exhaust heat recuperation technologies was performed in the Internal Combustion Engine Laboratory of NTUA (National Technical University of Athens). The evaluation was based on a comprehensive thermodynamic simulation model of diesel engines developed in this Laboratory. The simulation has been used to estimate exhaust gas characteristics and available amount of exhaust energy. In addition it was used, after modifications, to simulate turbocompounding both mechanical and electrical considering for the interaction between the T/C, the power turbine and the engine. The basic elements of this model are briefly outlined in this section.

2.1 Brief outline of the NTUA engine simulation model

The simulation covers the entire engine cycle taking into account the gas exchange period using the filling and emptying technique. It considers in general the following engine subsystems: a) Engine Cylinder b) Fuel Injection System and c) Gas Exchange System. It is based on a three-dimensional multi-zone combustion model. The pressure inside the engine cylinder is considered to be uniform. The first law of thermodynamics and the conservation equations for mass and momentum are employed for the calculation of local conditions inside each zone [1,2].

2.1.1 Heat transfer

A turbulent kinetic energy viscous dissipation rate $k\sim\varepsilon_t$ model is used to determine the characteristic velocity for the heat transfer calculations. The heat transfer coefficient is estimated from the following correlation [3,4],

$$h_c = c\,Re^{0.8}\,Pr^{0.33}\,\frac{\lambda}{l_{car}} \tag{1}$$

The overall heat exchange rate is then distributed among the zones according to their mass, temperature and specific heat capacity.

2.1.2 Air swirl

The swirling motion of the intake air is described in a rather simple, but quite efficient way assuming a hybrid scheme consisting of a solid body core surrounded by a potential flow region [3,5]. The intake air swirl velocity is estimated from the angular momentum conservation equation using the angular momentum added to the engine cylinder during the intake process and considering for the part destroyed because of friction with the combustion chamber walls. Details concerning the analysis are provided in [1,2].

2.1.3 Spray model

After initiation of fuel injection, zones form and penetrate inside the combustion chamber. The zone velocity along the jet axis is obtained from the following relations depending on the time instant after injection [1,6].

$$u_p = c_d\sqrt{\frac{2\Delta P}{\rho_l}} \quad \text{for } t<t_b \tag{2a}$$

$$u_p = \frac{2.95}{2}\left(\frac{\Delta P}{\rho_a}\right)^{0.25} d_{inj}^{0.5}t^{-0.5} \quad \text{for } t_b<t<t_{hit} \tag{2b}$$

$$u_p = \frac{2.95}{2}\left(\frac{\Delta P}{\rho_a}\right)^{0.25} d_{inj}^{0.5}t^{-0.5} \quad \text{for } t>t_{hit} \tag{2c}$$

where t_b is the breakup time and t_{hit} is the time of impingement on the cylinder walls. The breakup time is obtained from Jung and Assanis [7].

$$t_b = 4.351\frac{\rho_l d_{inj}}{c_d\left(\rho_a\Delta P\right)^{0.5}} \tag{3}$$

The effect of air swirl upon the jet is considered for, using the local components of the air velocity in the radial and axial directions and using the momentum conservation equations in both axes.

2.1.4 Air entrainment into the zones

The air entrained into a zone from initiation of injection is calculated from the conservation of momentum using the following relation:

$$m_f \cdot u_{inj} = (m_a+m_f)\cdot u_p \rightarrow m_a = (m_f \cdot u_{inj} / u_p - m_f) \tag{4}$$

2.1.5 Droplet break up and evaporation

The injected fuel is distributed to the zones according to the instantaneous injection rate, while inside each zone the fuel is divided into packages (groups) using a chi-squared distribution [3], where the droplets have the same Sauter Mean Diameter. For evaporation the model of Borman and Johnson [8] is followed, as described in [1-3].

2.1.6 Combustion model

The amount of air entering a zone is mixed with evaporated fuel. The local reaction rate depends on the local mass concentration of fuel, oxygen and the local temperature. Ignition commences after an ignition delay period, which is estimated using the local conditions inside the zone as follows [1-3,6]:

$$S_{pr} = \int_0^1 \frac{1}{a_{del} P_g^{-2.5} \Phi_{eq}^{-1.04} \exp\left(5000/T_g\right)} dt = 1 \tag{5}$$

where "Φ_{eq}" is the local equivalence ratio of the fuel air mixture inside the zone and a_{del} is a constant. After ignition the combustion rate of fuel is obtained from the following relation [1-3]:

$$m_{fb} = K_b C_f^{af} C_o^{ao} \exp\left(-\frac{E_c}{R_m}\right)\frac{1}{6N} \tag{6}$$

where K_b is a constant, E_c the reduced activation energy and C_f, C_o the mass concentrations of fuel and oxygen respectively. During diffusion combustion, the combustion rate is practically controlled from the air entrainment rate and it's mixing with evaporated fuel.

2.1.7 Fuel injection

The fuel injection system is of great importance for the operation of the diesel engine [3,9,10]. In the present work, the injection rate has been obtained from the following relation:

$$\frac{dm_{inj}}{dt} = C_{dinj} \cdot A_{inj} \cdot \sqrt{2 \cdot \Delta P \cdot \rho_f} \tag{7}$$

where: $\Delta P = P_{cyl} - P_{inj}$ is the instantaneous pressure difference at the nozzle exit, C_{dinj} the discharge coefficient, A_{inj} the area of the nozzle holes and ρ_f the fuel density. Since experimental injection rates were not available a constant rail pressure has been used during injection, which was estimated to match the measured injection duration at each operating condition.

2.1.8 Gas exchange

For the simulation of the inlet and exhaust manifolds and the calculation of the mass exchange rate between them and the engine cylinder the filling and emptying method is used. One-dimensional, quasi-steady, compressible flow is assumed for the calculation of the mass flow rates through the inlet and exhaust valves during the gas exchange process.

2.1.9 Turbocharger simulation

For the present simulation model T/C maps were used, provided by the T/C manufacturer for both mechanical and electrical turbocompounding. In the case of electric

turbocompounding the turbine effective flow area was calculated using an iterative procedure to provide the required exhaust pressure value before the turbine. Then the turbine excess power was estimated from the following relation:

$$P_{el,p} = P_{eT}\eta_{mT} - \frac{P_{eC}}{\eta_{mC}} \quad (8)$$

where P_{eC} is the compressor power, P_{eT} the power generated from the turbine and $P_{el,p}$ the excess power of the turbine which is then converted to electric power.
For the present application the mechanical efficiencies of the turbine and the compressor, n_{mT} and n_{mC} were taken equal to 0.95.

2.2 NTUA simulation model modification for turbocompounding

To consider for the existence of the power turbine, the NTUA engine simulation code has been undergone additional modifications. The power turbine has been mounted downstream of the existing T/C and its inlet conditions have been calculated using the first thermodynamic law and the power balance across the T/C. For this reason a new calculation procedure has been setup which estimates the pressure at the T/C turbine inlet to produce the required boost pressure that provides the necessary amount of air to the engine. For electrical turbocompounding, the main modification involved also the calculation procedure. A new methodology was developed al already mentioned to estimate the required turbine nozzle effective flow area to increase exhaust gas pressure before the turbocharger turbine to the required level [11]. Moreover, the simulation estimates the amount of turbine power required to drive the compressor and supply the necessary amount of air to the engine. Then the remaining amount of turbine power is the available one to be converted to electricity.
In both cases, the simulation estimates the total power produced from the system, which corresponds to the net engine power and the mechanical power produced from the power turbine or the electric generator in the case of electrical turbocompounding. The total power $P_{e,tot}$ produced is thus obtained from the following relation:

$$P_{e,tot} = P_{eE} + P_{eT,net}\eta_{GT} \quad (9)$$

where $P_{eT,net}$ is the power turbine power or the net power produced from the electric generator for electrical turbocompounding and P_{eE} is the net engine power. The term n_{GT} is the mechanical efficiency of the gear train for mechanical turbocompounding or the generator efficiency for electrical turbocompounding.

3. Mechanical turbocompounding

Mechanical turbocompounding refers to the addition of a power turbine after the T/C to extract mechanical power from the exhaust gas. Figure 1 depicts a representative schematic view of a diesel engine configuration equipped with an additional power turbine (Mechanical Turbocompounding). The power turbine is mounted downstream of the turbocharger (T/C) and is mechanically coupled to the engine crankshaft via a gear train. Caterpillar [11,12] used an axial power turbine on a 14.6-liter diesel and reported an average bsfc reduction of about 4.7% for a 50,000 miles extra-urban driving test in USA. Cummins [13] used a radial flow power turbine and achieved 6% improvement in bsfc at full load and

3% at part load. Finally, Scania [11] applied this technology on an 11-liter displacement 6-cylinder turbocharged diesel engine providing a 5% improvement of bsfc at full load.

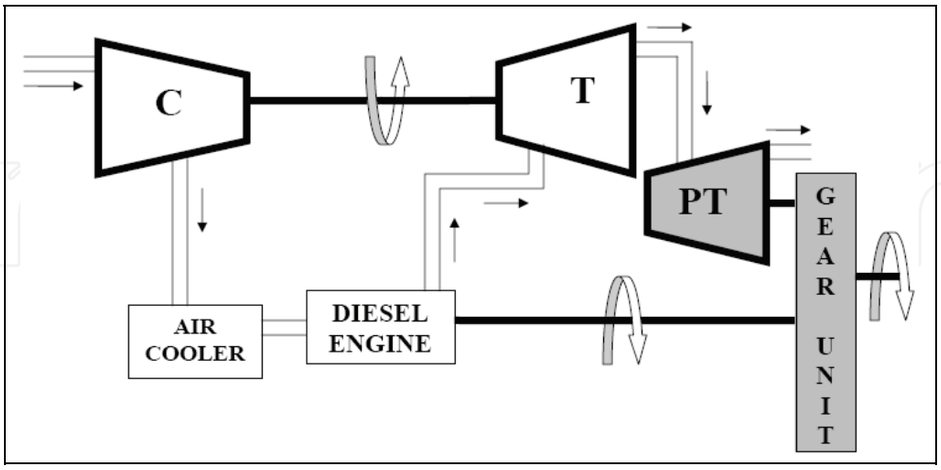

Fig. 1. Schematic view of Mechanical Turbocompounding.

Several theoretical studies have been conducted from various research groups to estimate the potential for exhaust heat recovery of a heavy-duty diesel engine when using mechanical turbocompounding. Using the model developed by the research group of NTUA-Internal Combustion Engines laboratory [1,2] a parametric investigation has been conducted using as a basis a diesel engine simulation model appropriately modified to consider for the effects of this technology [14]. The parametric investigation involved the effect of power turbine pressure ratio on engine performance and overall engine bsfc improvement. The power turbine pressure ratio has been varied in the range of 1.5-2.3. On the other hand, the power turbine efficiency has been kept constant at 80% The parametric analysis has been conducted for all engine-operating points shown in Table 1.

Speed (rpm)	**Load (%)**	**Fuel (kg/h/cyl)**	**Inlet Pressure (bar)**	**Injection Advance (deg ATDC)**
2100	25	3.00	1.36	-6
2100	50	4.87	1.78	-8
2100	75	6.90	2.06	-8
2100	100	8.77	2.20	-13
1700	25	3.45	1.50	-6
1700	50	6.10	2.23	-7
1700	75	8.90	2.65	-8
1700	100	11.80	3.08	-8
1300	25	3.25	1.61	-4
1300	50	5.87	2.36	-7
1300	75	8.83	3.01	-7
1300	100	12.00	3.73	-6

Table 1. Engine operating conditions considered for the investigation.

Before applying the simulation model for the examination of the various exhaust heat recovery techniques it has to be calibrated at a selected operating point. Its predictive ability concerning engine performance and emissions is also validated afterwards against available experimental data. This is a standard procedure when using a simulation model and is always performed before it is used in any theoretical investigation.

3.1 Effect on engine performance and potential bsfc improvement

The parametric analysis of mechanical turbocompounding is conducted considering a variation of power turbine pressure ratio from 1.5 to 2.3. The effect of this variation on exhaust manifold pressure is depicted in Fig. 2 for all engine loads at 1700 rpm engine speed. The maximum value of exhaust pressure is 5.76 bar at full engine load for the maximum power turbine pressure ratio. On the other hand the maximum pressure ratio is obviously lower and in the range of 2.6-2.7 which is quite acceptable.

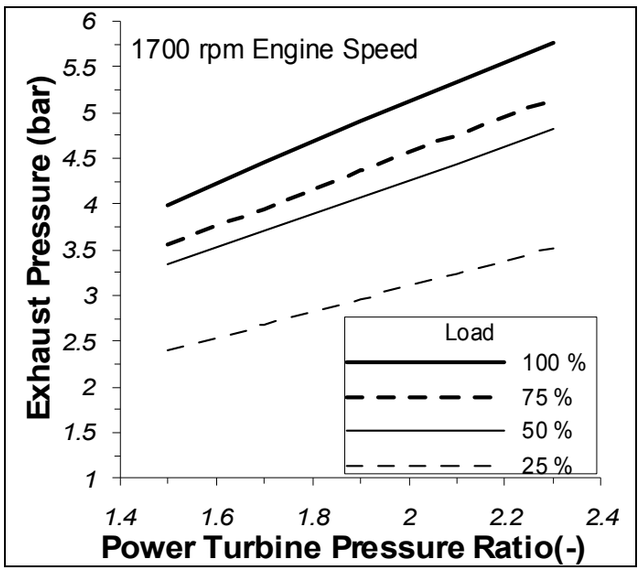

Fig. 2. Exhaust Pressure variation vs. power turbine pressure ratio at 1700 rpm for various engine loads.

During the parametric analysis, the fuelling rate for turbocompounding has been maintained constant. Therefore to estimate its effect on engine bsfc it has been considered the overall power output i.e. the power generated from the engine and the power turbine. In Fig. 3 is given the percentage change of overall engine bsfc vs. power turbine pressure ratio at 1700 rpm for loads ranging from 25% to 100%. As revealed, the introduction of mechanical turbocompounding results to a decrease of overall bsfc. In general the relative reduction of bsfc increases initially sharply with power turbine pressure ratio and then after a certain point the increase starts to decline. For part load operation after a certain pressure ratio bsfc improvement starts to decrease revealing that a maximum has been reached. Therefore, the optimum pressure ratio is shifted to higher values of power turbine pressure ratio with the increase of engine load. As depicted in Fig 3, the potential of bsfc decrease is extremely low at 25% load and increases to approximately 4.5% at full load. It is also noticeable that after a certain power turbine pressure ratio at medium and high loads the additional decrease of bsfc is rather limited while it has a negative effect on exhaust pressure

as shown in Fig. 2. Therefore considering the overall results it appears that the overall optimum power turbine pressure ratio is in the range of 1.7-1.9.

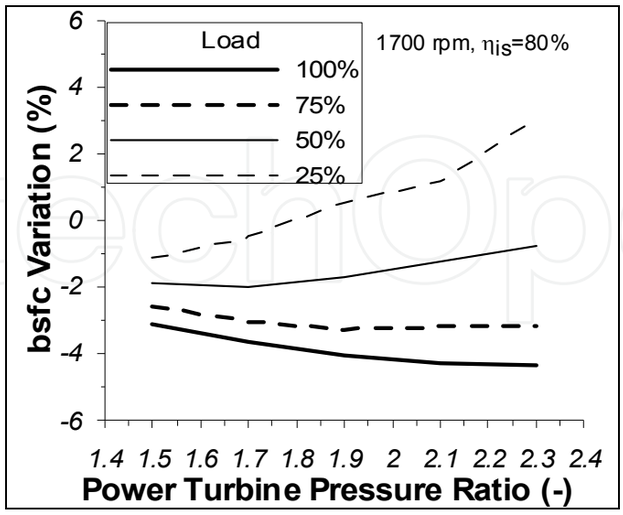

Fig. 3. bsfc variation vs. power turbine pressure ratio at 1700 rpm for various engine loads.

Another important issue is the effect of mechanical turbocompounding on engine power output. An increase of exhaust pressure before the T/C turbine (Fig. 1) is observed due to the addition of the power turbine. Due to this, gas exchange work is increased which is expected to have a negative impact on net engine power. This is verified by Fig. 4 providing the relative reduction of engine power output with power turbine pressure ratio for all loads examined. As observed, engine power decreases almost linearly with increasing power turbine pressure ratio the slope increasing with the reduction of engine load. The engine power reduction considering the previous value of the optimum pressure ratio (1.7~1.9) ranges from 8% at 100% load to 20% at 25% load. The absolute reduction of primary engine power is depicted in Fig. 5. As shown, net engine power decreases from 352 kW to 325 kW at full engine load linearly with power turbine pressure ratio the slope being the same for all engine loads.

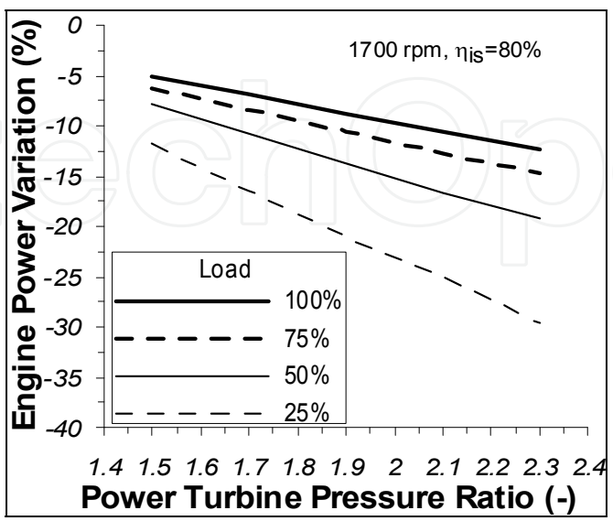

Fig. 4. Engine power variation vs. power turbine pressure ratio at 1700 rpm and various engine loads.

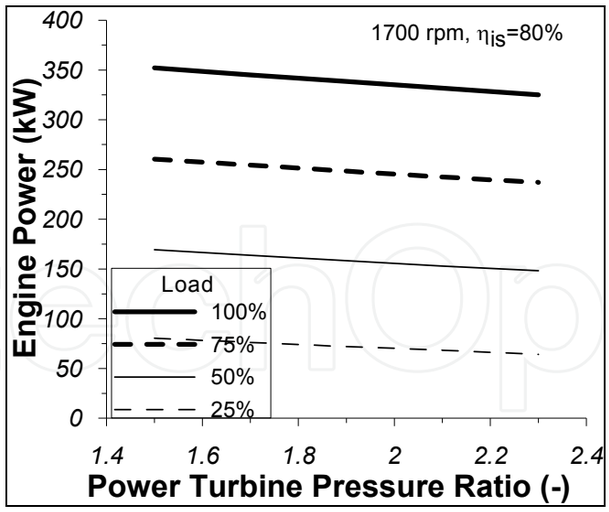

Fig. 5. Net engine power vs. power turbine pressure ratio at 1700 rpm and various engine loads.

On the other hand, in Fig 6 is given the variation of generated power at the power turbine vs. pressure ratio for all loads examined. It is observed an increase of generated power with increasing pressure ratio the slope decreasing with the increase of pressure ratio. The slope of the curve, as expected increases also with engine load and a maximum generated power value of approximately 35 kW is expected if the pressure ratio is maintained in the optimum range of 1.7~1.9.

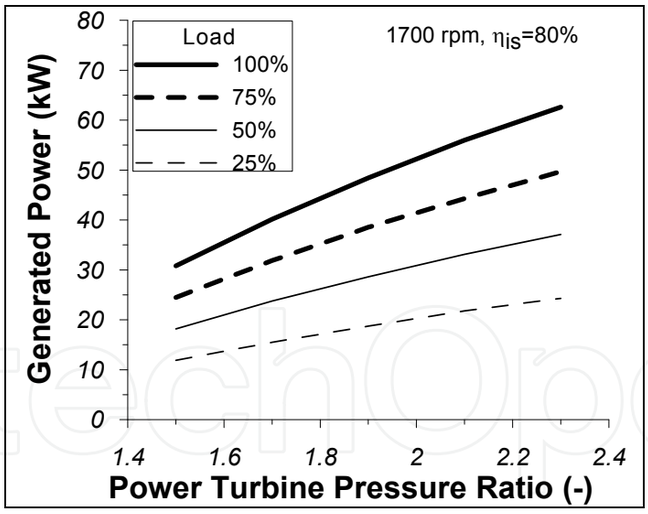

Fig. 6. Generated Power vs. power turbine pressure ratio at 1700 rpm and various engine loads.

4. Electrical turbocompounding

Electrical turbocompounding (Fig 7) recuperates part of the exhaust gas heat directly from the T/C using a high-speed generator. In this case the turbine produces more power compared to the one required to drive the compressor. This excess power is converted to electric power using a high speed generator incorporated into the TC casing. Caterpillar has considered this concept in a research program [15-16] providing indications for 5%

reduction of bsfc on a cycle basis and a maximum reduction of approximately 9-10% when using turbocharger components with high efficiency.

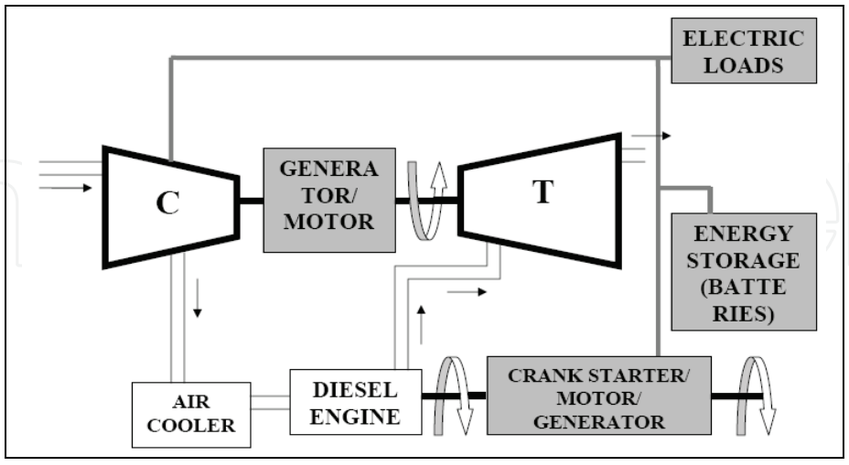

Fig. 7. Schematic view of Electrical Turbocompounding.

Using the NTUA engine simulation model described in section 2 a parametric investigation similar to the one conducted for mechanical turbocompounding has been conducted also for the case of electrical turbocompounding. The engine operating conditions examined are again the ones displayed in Table 1. However in the present investigation the parameters examined were turbocharger efficiency and exhaust pressure increase before the turbine. The investigation has been conducted for three values of overall T/C efficiency, i.e. the standard value corresponding to the provided T/C maps and two additional ones considering an increase of 10% and 20% on a percentage basis. For the standard T/C the maximum overall efficiency is approximately 49%, for the one with a 10% increase 54% and for the last with a 20% increase 60%. The last value i.e. 60% corresponds to an isentropic efficiency of both turbine and compressor in the range of 80% that can be considered realistic especially for future improved T/Cs.

In the case of electric turbocompounding, exhaust pressure has been increased approximately 1 bar above the value corresponding to the non-turbocompound case using the standard T/C efficiency. Obviously the potential for exhaust pressure increase is higher when using a T/C with increased efficiency. The value of 1 bar exhaust pressure increase has been selected to avoid excessive pressure ratios across the turbine of the turbocharger.

4.1 Effect on engine performance and potential bsfc improvement

During the investigation exhaust pressure has been increased approximately 1 bar above the one corresponding to the standard efficiency T/C. In Fig.8 are given the corresponding values of exhaust pressure for the standard efficiency T/C vs. exhaust pressure increase for 25% and 100% load. From this graph it appears that the maximum pressure ratio across the turbine is 4.0 which is high and explains the reason for increasing exhaust pressure only by 1 bar. Obviously the absolute exhaust pressure value compared to mechanical turbocompounding, Fig. 2 is significantly lower.

The effect of electrical turbocompounding on engine performance is given as function of turbine inlet pressure variation (compared to the standard value). To estimate bsfc improvement in this case, two different approaches are adopted, one by comparing bsfc

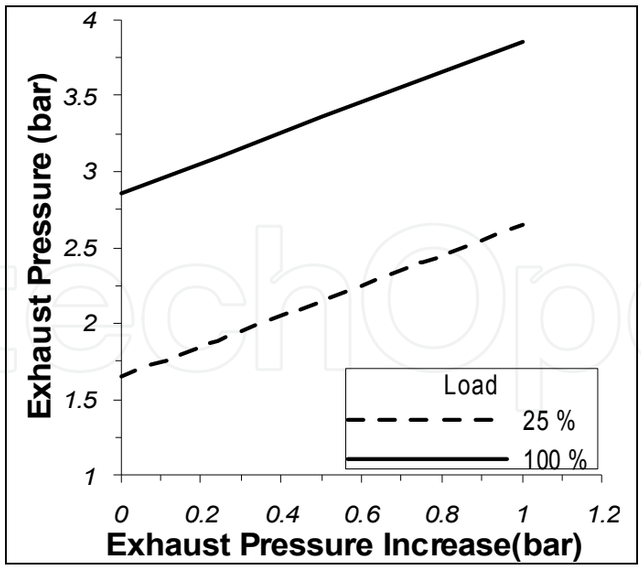

Fig. 8. Exhaust manifold pressure variation vs. exhaust pressure increase for 1700 rpm and 25% load.

variation to the non-turbocompound case for each T/C efficiency considered and a second by comparing the non-turbocompound case to the standard T/C efficiency (existing one). In the first case the actual benefit of electrical turbocompounding is revealed while in the second the result is the combined effect of both electrical turbocompounding and increased T/C overall efficiency.

In Figs 9a,b and 9c,d is given the overall bsfc change vs. exhaust pressure variation for 25% and 100% load respectively for the two approaches adopted. As observed, a different behavior is revealed at 25% and 100% load, Figs 9a,b and 9c,d respectively. At low engine load, the bsfc reduction is significantly lower compared to the one at full engine load.

In Fig 9a is depicted the bsfc variation compared to the one without turbocompounding and the current T/C efficiency at 25% load. As revealed, bsfc improvement starts to deteriorate after a certain value of exhaust pressure increase, which is shifted towards higher values as T/C efficiency increases. On the other hand in Fig.9b is given the bsfc variation compared to the non-turbocompound case for the standard T/C efficiency. Obviously in this case bsfc reduction is significantly higher. The observed maximum bsfc improvement attributed to electric turbocompounding alone is 1% for the highly efficient T/C efficiency while the total bsfc improvement due to both turbocompounding and increased T/C efficiency is 3.5%.

For 100% load, Figs 9c,d., bsfc reduction continues to improve with exhaust pressure increase the slope of the curve being reduced as exhaust pressure increases. The maximum bsfc improvement attributed to electric turbocompounding alone is 5% for the highly efficient T/C. On the other hand the total overall bsfc improvement due to both electric turbocompounding and increased T/C efficiency is 6.5%. Therefore a considerable bsfc improvement especially at low and medium load is experienced only using a high efficiency T/C. At 25% load the maximum bsfc improvement is attributed by 2/3 to T/C efficiency increase and by 1/3 to turbocompounding. At high load the situation is reversed and the overall improvement is attributed by 1/3 to T/C efficiency increase and 2/3 to electric turbocompounding. Therefore, the previous analysis reveals that electrical turbocompounding can be beneficial if we use a highly efficient T/C. Consequently the need for increasing T/C efficiency is clearly revealed.

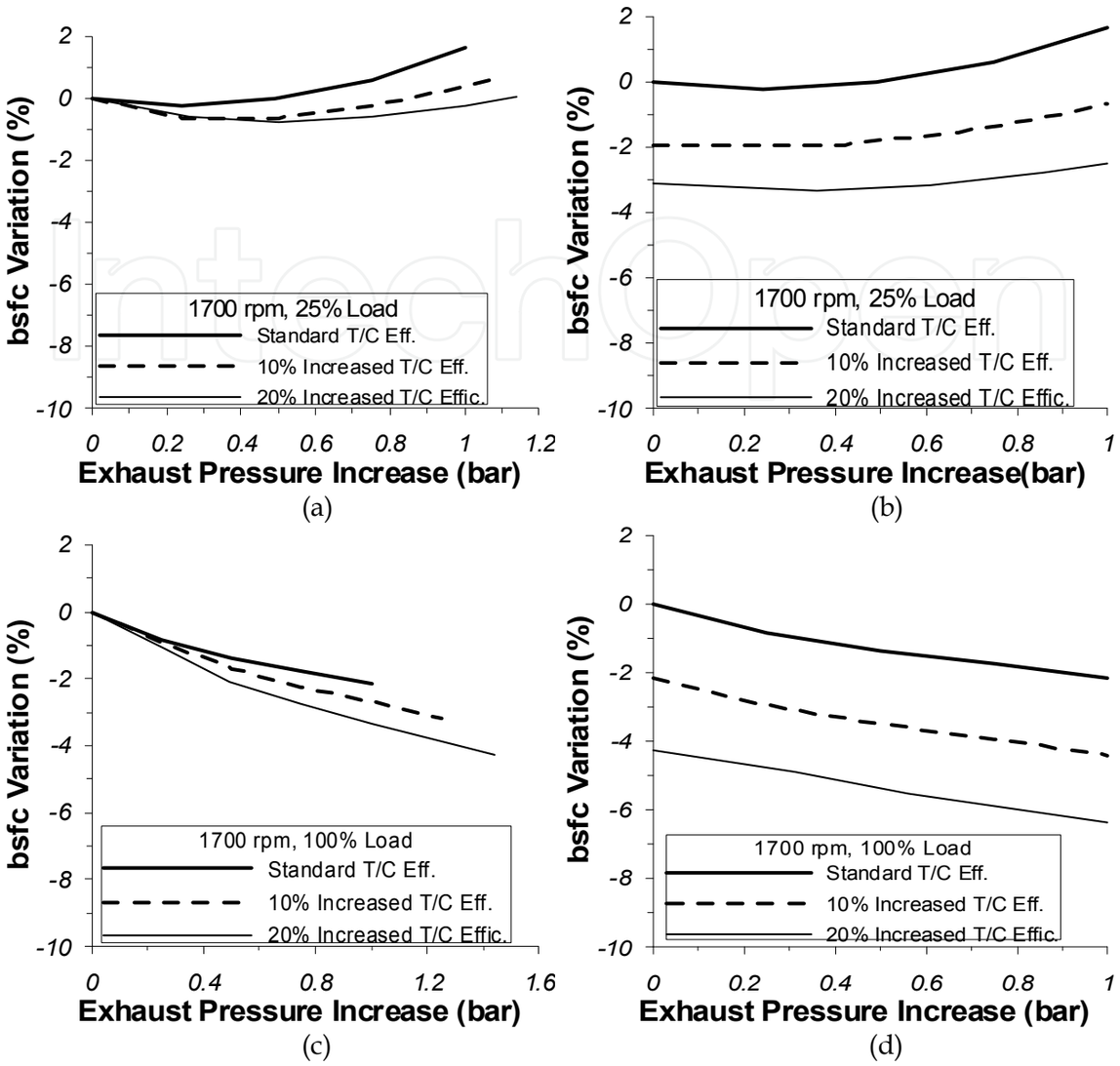

Fig. 9. (a) bsfc variation vs. exhaust pressure increase for 1700 rpm and 25% load. (b) bsfc variation compared to the standard T/C efficiency vs. exhaust pressure increase for various T/C efficiencies at 1700 rpm and 25% load. (c) bsfc variation vs. exhaust pressure increase for 1700 rpm and 25% load. (d) bsfc variation compared to the standard T/C efficiency vs. exhaust pressure increase for various T/C efficiencies at 1700 rpm and 100% load.

In the case of electric turbocompounding, generated electric power is significantly important because it defines the size of the required electric generator. As witnessed from Figs 10a-b corresponding to 25% and 100% load generated electric power increases with exhaust pressure at a decreasing slope. Generated electric power increases significantly with the increase of T/C efficiency. For the case examined the maximum generated electric power ranges from 15 kW at 25% engine load to 40 kW at 100% engine load for the highly efficient T/C.

Finally, in Figures 11a-b is given the relative decrease of net diesel engine power for 25% and 100% respectively as function of exhaust pressure increase. The relative decrease has a maximum value of 18% at low engine load and 6% at full engine load. The relative reduction of net engine power does not depend on T/C efficiency and varies linearly with

exhaust pressure increase. Compared to mechanical turbocompounding the relative reduction is lower since a lower exhaust manifold pressure has been used as already shown.

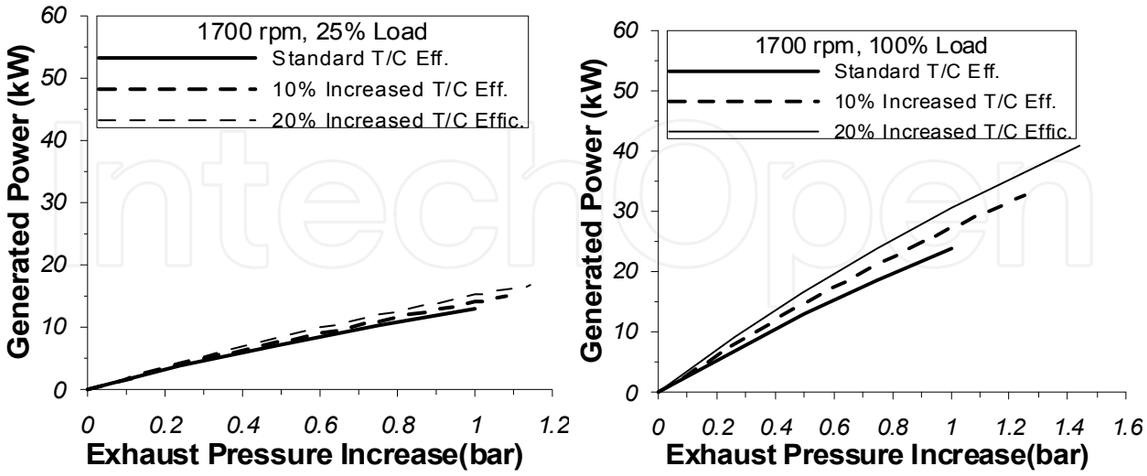

(a) (b)

Fig. 10. (a) Variation of Generated Power vs. exhaust pressure increase at 1700 rpm and 25% load for various T/C efficiencies. (b)Variation of Generated Power vs. exhaust pressure increase at 1700 rpm and 100% load for various T/C efficiencies.

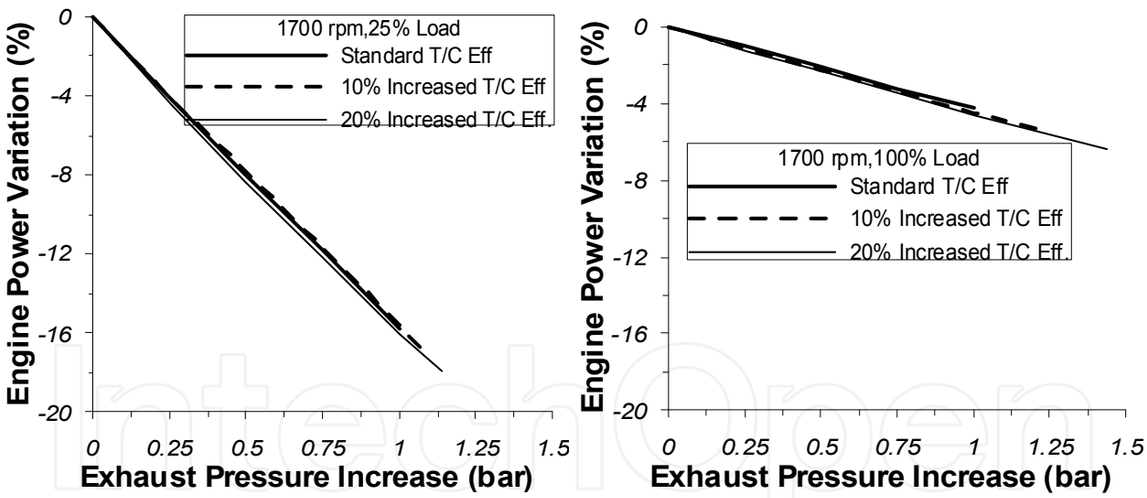

(a) (b)

Fig. 11. (a) Relative decrease of net engine power vs. exhaust pressure increase at 1700 rpm and 25% load for various T/C efficiencies. (b) Relative variation of net engine power vs. exhaust pressure increase at 1700 rpm and 100% load for various T/C efficiencies.

5. Implementation of Rankine cycle

5.1 General description

In the case of heavy duty diesel engines, suitable for truck applications, one of the most promising technical solutions for exhaust gas waste heat utilization appears to be the use of

a "Bottoming Rankine Cycle" [17,18]. A systematic approach for the use of Rankine Cycle installation for truck applications is dated back in the early 70's where a research program funded by US Department of Energy (DOE) was conducted by Mack Trucks and the Thermo Electron Corporation [19-21]. During this program, an Organic Rankine Cycle System (ORCS) was installed on a Mack Truck diesel engine. Lab test results revealed a peak bsfc improvement of 10% to 12.7% which as claimed was verified from highway tests even though no detailed additional information was provided. During the next years similar research programs were performed by other research institutes and vehicle manufacturers [22,23]. However, recently the solution of Rankine Cycle systems has increased its potential competitiveness in the market [24-27]. This is the result of technical advancements in a series of critical components for the operation of such an installation (heat exchanger, condenser, expander etc.), the highly increased fuel prices and the global thermal problem. Due to the last two, the installation and use of a Rankine Cycle is not only considered nowadays as a feasible solution for efficiency improvement of heavy duty truck diesel engines [28,29] but also for smaller applications i.e. passenger cars [30].

As expected the introduction of such an advanced concept in today's HD diesel engine technological status apart from the benefits creates several problems that have to be attained and resolved during the early design stage in a competitive way so that the concept retains its feasibility. One of the most important issues [26,27] is packaging of the additional devices and components within the existing engine and within the available space on a truck. However the increment of the bsfc of the new system (Rankine cycle and diesel engine) at a typical amount of 10% triggers automatically the need to reject increased amounts of heat to the environment through the low temperature reservoir system (condenser, engine radiator in the present case). Studies performed up to date by the authors [14] and other research groups [25-27,31] have demonstrated that when a Rankine cycle is coupled to an existing truck engine installation the use of a larger radiator, compared to the existing one, is necessary. The limitations for the dimensions of the radiator installed on a truck are clear and as a consequence the use of a second radiator appears a feasible solution to cover the increased heat rejection because of the bottoming cycle [32].

A representative layout of this technology is provided in Fig 12, where an exhaust gas heat exchanger is employed after the turbocharger turbine to provide heat to the Rankine cycle working medium. The Rankine cycle system includes an expander which drives a "feeder" pump and a fan mounted on the rear of the radiator-condenser.

The thermodynamic processes in a Rankine cycle are the following: The working medium enters the circulation (feeder) pump at the saturated liquid state and exits at the high pressure p_H. Then the working medium flows into the exhaust gas heat exchanger where it is preheated from the subcooled region at the exit of the pump to the saturated liquid state. As depicted in Fig. 12 the required thermal energy for working medium evaporation and superheating is covered by the main exhaust gas stream and partially by EGR heat. Utilization of EGR heat is favorable for cycle efficiency because of its superior thermodynamic characteristics (i.e. higher temperature level). The superheated vapor expands from the high pressure p_H to the lower pressure p_L. Finally, the expanded working medium is condensed and heat is rejected to the ambience. The working fluid at its saturated liquid state enters the pump.

A variety of working media have been considered during Rankine cycle applications. They are typically separated in two main categories: i.e. water (steam) and typical organic media

(like R245ca). In an effort to reduce the dimensions of the Rankine system one of the basic ideas is the utilization of heat from other sources apart from the exhaust gas which is rejected to the environment during normal engine operation. In existing and future heavy duty diesel engine applications such sources for additional heat recuperation are CAC (Charge Air Cooler) and most likely EGR (Exhaust Gas Recirculation) Cooler Heat [31]. Significant amounts of heat are expelled to the ambient from both devices during the operation of a HD truck engine. Using the simulation models developed, it is clearly demonstrated the potential benefits arising for both system efficiency and reduction of radiator dimensions when heat from these additional energy sources is utilized.
Finally using models developed especially for the simulation of the heat exchange processes taking place in a HD diesel truck radiator estimation can be performed for the geometrical dimensions of both the diesel engine and Rankine cycle radiators that are necessary to fulfill the heat rejection demands of the installation. Different radiator arrangements have also been investigated to propose an optimized solution with minimum radiator surfaces considering for the cooling air mass flow rate.

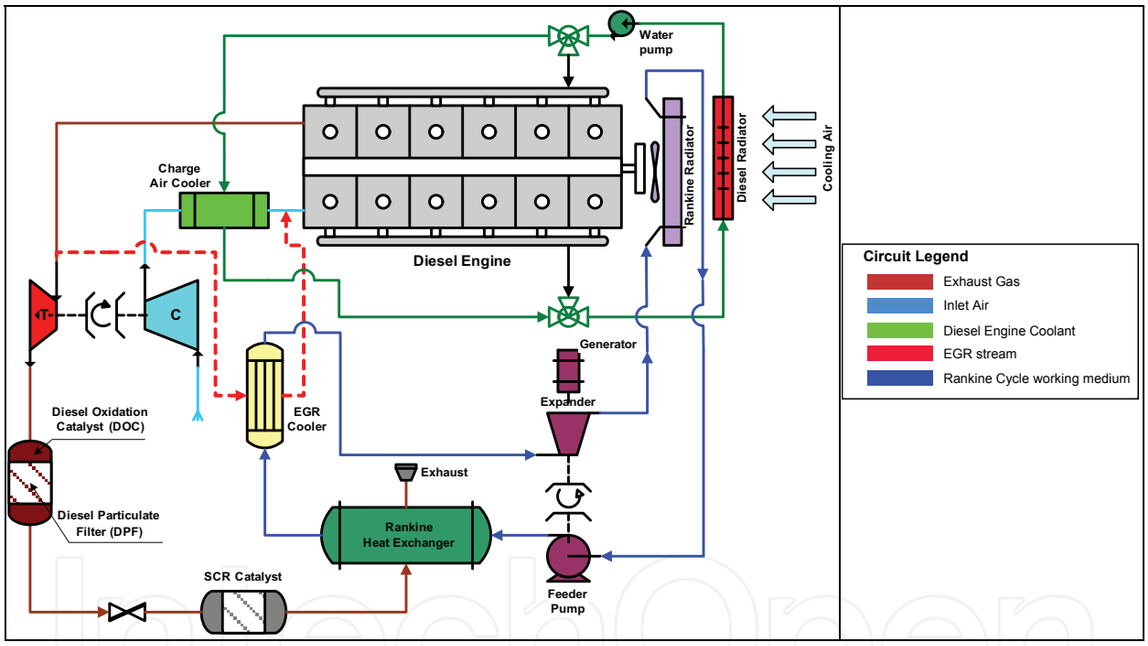

Fig. 12. General layout for the arrangement of the Rankine cycle system components on a HD DI Diesel engine installation.

5.2 Simulation model for the Rankine cycle

A detailed simulation model has been developed by the authors in NTUA for the evaluation of the Rankine cycle system which is used to recover energy from the exhaust gas and other sources of waste heat available in the diesel engine installation examined. The required thermodynamic and transport properties for the water and organic working medium have been calculated from "REFPROP", an electronic database developed by NIST (National Institute of Science and Technology) [33]. The exhaust gas properties have been calculated using polynomial expressions. On the other hand the exhaust gas composition is estimated from the diesel engine simulation (described in section 2). The various components of the

Rankine cycle have been simulated by developing appropriate sub-models based on the basic principles of thermodynamics and heat transfer [34].
Two cases for exhaust gas heat recuperation have been examined. The first is the basic configuration where heat is recovered only from the main exhaust gas. In the second it is considered the simultaneous heat recovery from the main exhaust gas stream (from the Rankine main heat exchanger), the recirculated exhaust gas stream (existing EGR cooler) and the charge air stream after the compressor (existing charge air cooler, CAC). The Rankine heat exchanger used for heat recuperation in all cases is of the shell and tube type with two tube passes.
One of the most important targets of the simulation is to estimate the optimum design of the Rankine cycle at each engine operating point to achieve the maximum efficiency gain. For this reason, a parametric analysis is performed at each operating point examined where the key parameter is Rankine cycle high pressure P_H The second parameter of the study is the superheated vapor temperature T_{win_exp} before the expander. The minimum value of temperature T_{win_exp} is carefully selected to secure that the working media after expansion has a vapor content above 90% which is accepted as the upper limit (max. liquid content 10%) for the safe operation of a reciprocating expander. The minimum value of superheated vapor temperature obviously depends on the Rankine cycle high pressure P_H.
All components of Rankine cycle are simulated based on their basic thermodynamic and heat transfer principles. Thus the model includes the following elements:

- Simulation of Exhaust Gas Heat Exchanger, EGR Cooler and Charge Air Cooler
- Expander Simulation
- Simulation of the Circulation Pump
- Calculation of Rankine Cycle Performance and Overall Energy Balance
- Simulation Model for System Radiators

5.3 Effect of the Rankine cycle on engine power and efficiency improvement

The investigation for both steam and organic has been conducted at 1700 rpm engine speed at four different loads ranging from 25%-100%. This covers the investigation for overall system performance, the effect of EGR and CAC heat utilization on total bsfc and heat exchanger size. The set of engine operating points considered in the present investigation together with the values of several characteristic operating parameters are presented in Table 2. Additionally, in Table 3 are presented the respective heat amounts rejected to the ambience during normal diesel engine operation.

Engine Speed (rpm)	Engine Load (%)	Power (kW)	$\dot{m}_{exh}$ (kg/s)	$\dot{m}_{EGR}$ (kg/s)	λ (-)	P_{EGR} (bar)	T_{exh_in} (^oC)	T_{EGR_in} (^oC)	T_{AIR_in} (^oC)
1700	100	366.6	0.4945	0.0982	1.5404	4.14	397.8	581.0	201.46
1700	75	277.8	0.4058	0.1046	1.6410	3.87	354.3	518.2	180.42
1700	50	183.6	0.2993	0.1314	1.6930	3.79	306.6	455.3	161.17
1700	25	90.0	0.1784	0.1194	1.7781	2.47	285.3	383.4	111.13

Table 2. Engine operating conditions considered for the present investigation.

Engine Speed (rpm)	Engine Load (%)	$\dot{Q}_{COOLANT}$ (kW)	$\dot{Q}_{REJ\_EGR}$ (kW)	$\dot{Q}_{REJ\_AC}$ (kW)	$\dot{Q}_{TOT}$ (kW)
1700	100	130.0	46.0	93.8	269.8
1700	75	109.6	41.8	69.6	221.0
1700	50	88.6	43.4	47.0	179.0
1700	25	57.8	30.0	18.8	106.6

Table 3. Engine heat amounts rejected to the environment.

The main questions that arise after the introduction of the Rankine cycle in a heavy duty diesel truck refer to the expected efficiency improvement of the new power plant and the additional mechanical power that the new system is capable to provide. In the present work it is examined the effect of EGR gas and charge air heat utilization on both parameters. The results for steam are given in Figs 13 and 14 (a-b) at 1700 rpm engine speed and three engine loads namely 50, and 100% (a-b). In Fig. 13 are given the results without EGR and CAC heat utilization and in Fig. 14 the corresponding ones when both EGR cooler and CAC heat amounts are partially utilized as function of the cycle high pressure In the same figures is given the variation of the total heat amount absorbed from the Rankine cycle system vs high cycle pressure.

From Figs 13 and 14 it is observed an improvement of the overall efficiency of the Rankine-Engine power plant (reduction of specific fuel consumption) when compared to the diesel engine under the same conditions. The bsfc improvement increases slightly with engine load (from a to b) in both cases presented in Figs 13 and 14. The maximum bsfc improvement for steam at 1700 rpm is observed at 100% load case and is approximately ~ 5.5% when heat is extracted only from the main exhaust gas stream. However it should be noted that a higher bsfc reduction has been observed at 1300 rpm engine speed estimated at ~ 8-8.5% (where exhaust gas temperature characteristics are more favorable). But when heat from the EGR and CAC is utilized in the Rankine cycle, then bsfc reduction for the present operating condition (i.e. 1700 rpm, 100% load) is increased by approximately 40-50% to ~ 9% (absolute value). This trend is maintained almost the same for the entire engine operation field. The corresponding respective increase in net power benefit from the Rankine cycle is obviously similar and is ~40-50% higher with the recuperation of heat from EGR and CAC at full and part load respectively. From these results it becomes obvious that the contribution of both EGR and CAC coolers to the total amount of recuperated heat is significant.

As Rankine cycle high pressure increases, it would be expected a continuous increase of both bsfc improvement and generated power because of Rankine Cycle efficiency improvement. However, from the results of Figs 13 and 14 it is obvious that this is not the case. The reason is that the increase of cycle high pressure favors Rankine Cycle efficiency but on the other hands makes heat exchange between the working medium and the exhaust gas stream more difficult. As a result generated power output and thus bsfc reduction remain fairly constant after a certain high pressure and even start to decline at very high values. This trend is more obvious in Fig. 14 (a-b) where the EGR and CAC heat amounts are introduced into the system. The utilization of both EGR and CAC heat amounts makes it possible to extend considerably the Rankine cycle high pressure range which is favorable as for reduction of heat rejection, without negative impact on bsfc reduction potential.

The effect of cycle high pressure increase on bsfc improvement and Rankine cycle generated power is easily explained if we consider that the thermodynamic properties of the exhaust gas remain constant while the ones of the working medium (pressure, temperature) during

the various phases (preheating, evaporation, superheating) increase. The increase of working medium temperature reduces the amount of heat which can be extracted from the exhaust gas as displayed in Figs 13 and 14 (a-b). Thus the increase of Rankine cycle efficiency, through the increase of cycle high pressure, has a simultaneous negative impact on the heat transfer mechanism between the exhaust gas and working medium (steam in the present case) since the temperature difference between them is decreased. The combination of these two reverse trends results to a neutral effect on overall system bsfc and generated power after a certain cycle high pressure.

Therefore from the simulation it is revealed that the use of a cycle high pressure value above the optimum one for bsfc improvement and generated power could be considered for the reduction of rejected heat especially at high load where the capacity of engine cooling system may be exceeded.

The corresponding results for 1700 rpm engine speed concerning Rankine cycle net power, efficiency (bsfc reduction) and total heat absorbed when R245ca organic working medium is used are displayed in Figs 15 and 16 (a-b). Figure 15 provides results for the case without EGR and CAC heat utilization while Fig. 16 provides the corresponding results when these heat amounts are partially utilized. In this case it is observed that the potential efficient improvement offered by the Rankine cycle (reduction of specific fuel consumption) is higher compared to steam. The difference in efficiency improvement compared to steam is ~1% in absolute units for the case without utilization of EGR and CAC heat. However when these heat amounts are partially utilized the difference is increased to 3% in absolute units at the same conditions. This is the result of the organic media thermodynamic properties which favors heat exchange from the charge air, that has a relatively low temperature, to the working fluid.

It should also be mentioned that the mass flow rate of the organic media is approximately 10 times higher compared to steam, at the same operating conditions, due to the significant differences of physical properties between the two substances. This makes possible the use of a turbine expander instead of a reciprocating one which appears to be favorable as far as packaging and cost is concerned.

As in the case of steam, efficiency improvement for R245ca increases with the increase of engine load (Figs 15 and 16 a-b) and the maximum bsfc improvement observed for 100% load is ~ 11.3% when both EGR and CAC heat amounts are partially utilized (Fig 16b). Compared to the case where EGR and CAC heat is not utilized both efficiency gain and generated power are increased by ~50% (this value is even exceeded at part load operation). Therefore, as in the case of steam, the contribution of EGR and CAC heat to the total recuperated amount is significant.

As mentioned, there exist significant differences in the thermo physical properties between steam and organic working medium. Of special interest is the opposite inclination of the saturation curve of the organic R245ca in the vapor area compared to steam, which provides higher flexibility for the thermodynamic conditions at the expander inlet since at the end of the expansion stroke the organic medium is always inside the vapor area. Thus there is no possibility for condensate formation inside the expander which allows initiation of the expansion stroke at a position favoring the remaining thermodynamic phases of the Rankine cycle.

However the limitation concerning the increasing difficulty of heat transfer with the increase of cycle high pressure (vaporization pressure), which has been already described, is still valid. Observing the corresponding results provided in Figs 15 and 16 (a-b) it is obvious that this effect exists but is not so intense due to the low critical pressure for R245ca ~ 39.25 bar which does not allow variation of high pressure up to the point where generated power

will start to decline. As already mentioned supercritical cycles are not within the scope of the present analysis, even though they are interesting, because they require further considerations that are not within the scope of the present investigation. However they will be the subject of future work from the present research group.

From the results of the present work (Figs 15 and 16 it is concluded that for the organic medium considered the vaporization pressure should be kept at its highest possible level (below the critical) at any operating condition regardless of the utilization of EGR and CAC heat.

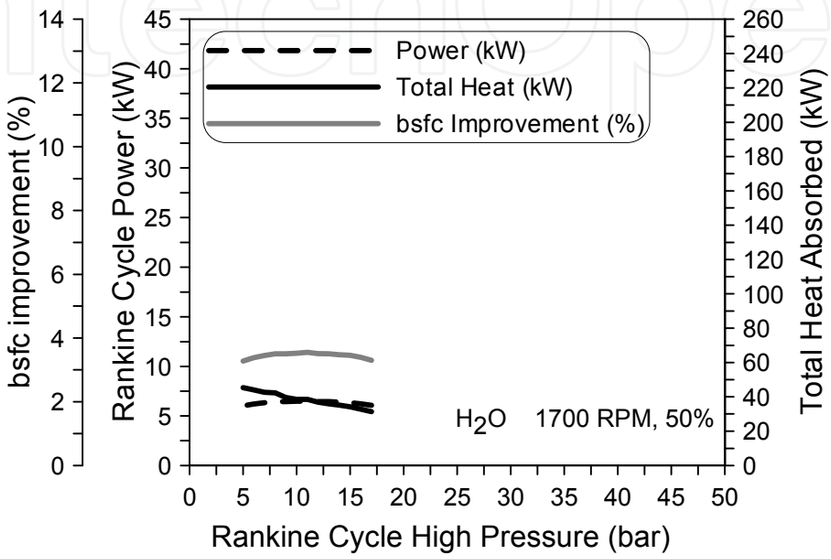

(a)

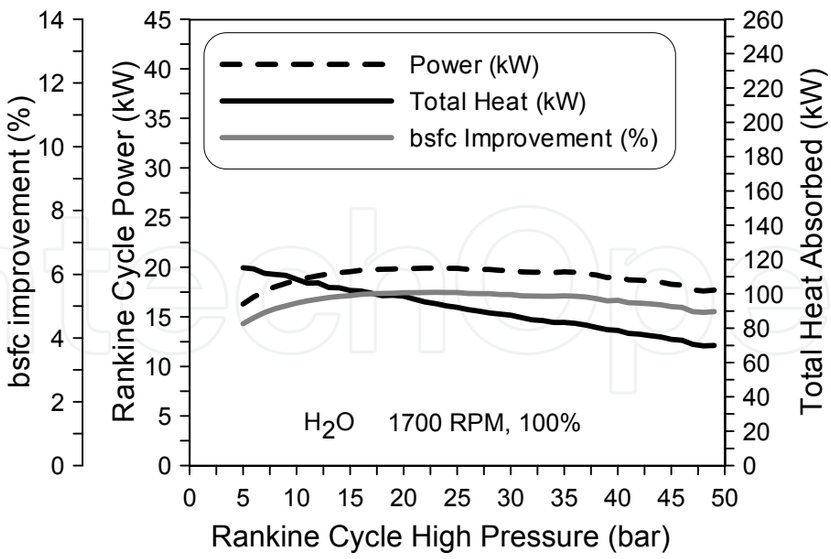

(b)

Fig. 13. bsfc improvement, generated power and total recuperated heat vs cycle high pressure, for 1700 rpm engine speed and three different loads 50% (a) and 100% (b) without EGR and CAC heat utilization.

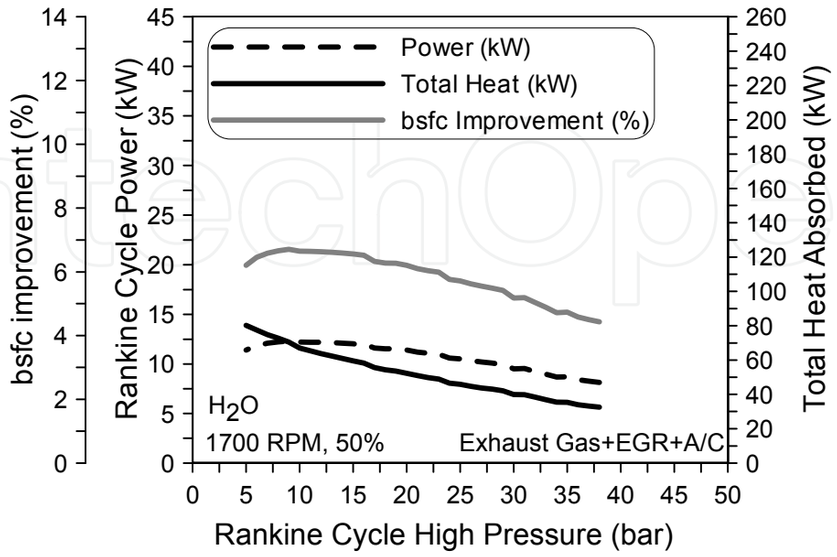

(a)

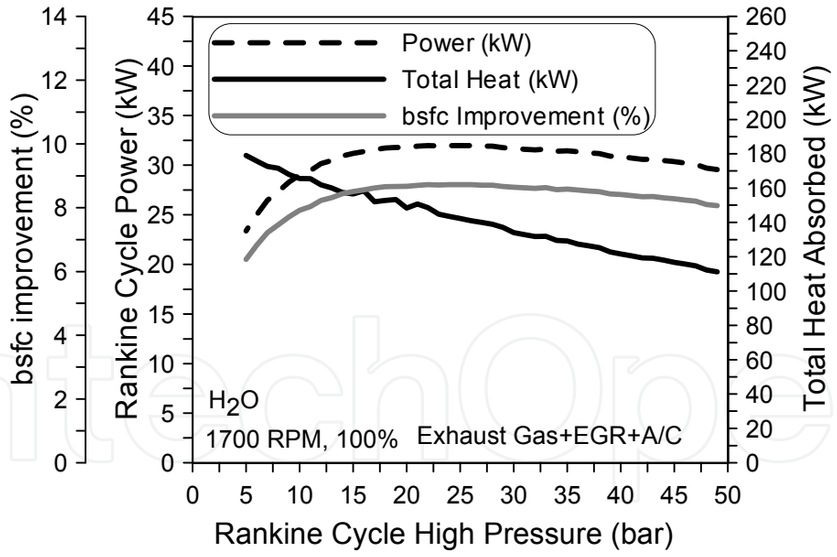

(b)

Fig. 14. bsfc improvement, generated power and total recuperated heat vs cycle high pressure, for 1700 rpm engine speed and three different loads50% (a) and 100% (b) with partially utilized EGR and CAC heat.

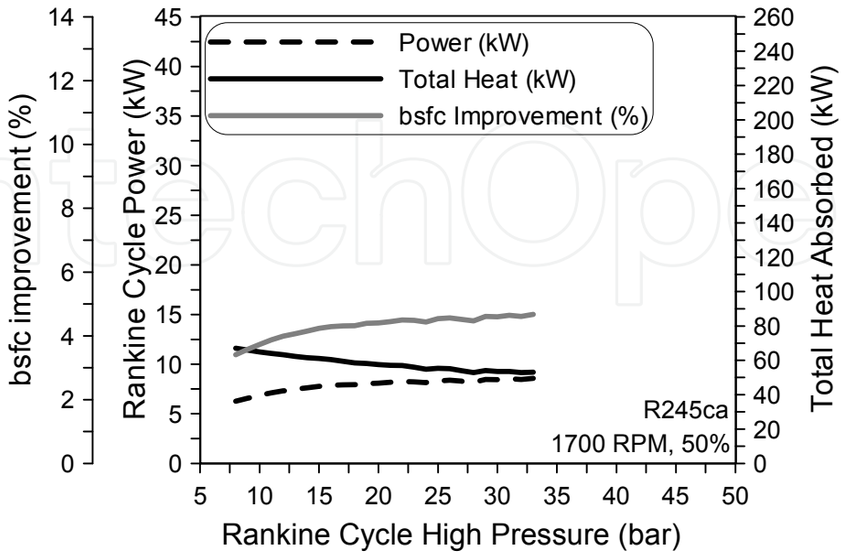

(a)

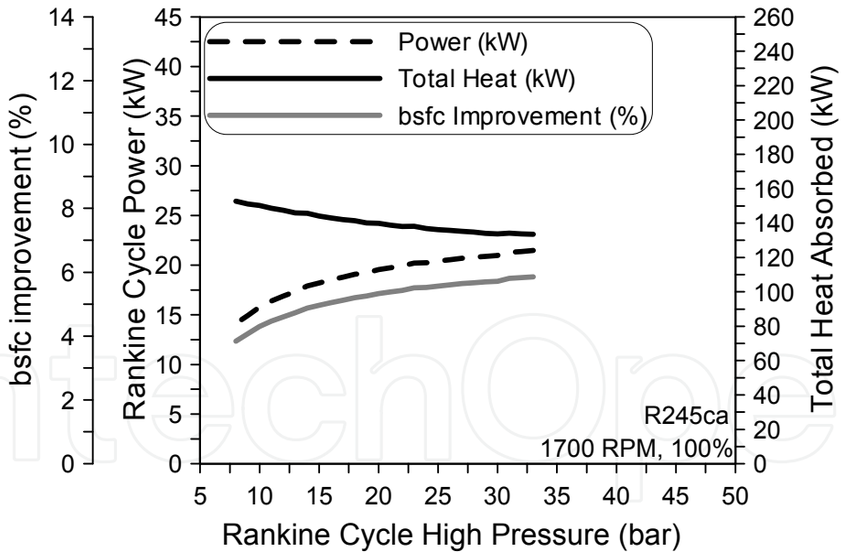

(b)

Fig. 15. bsfc improvement, generated power and total recuperated heat absorbed by the organic (R245ca) Rankine cycle vs cycle high pressure, for 1700 rpm engine speed and three different loads 50% (a) and 100% (b) without EGR and CAC heat utilization.

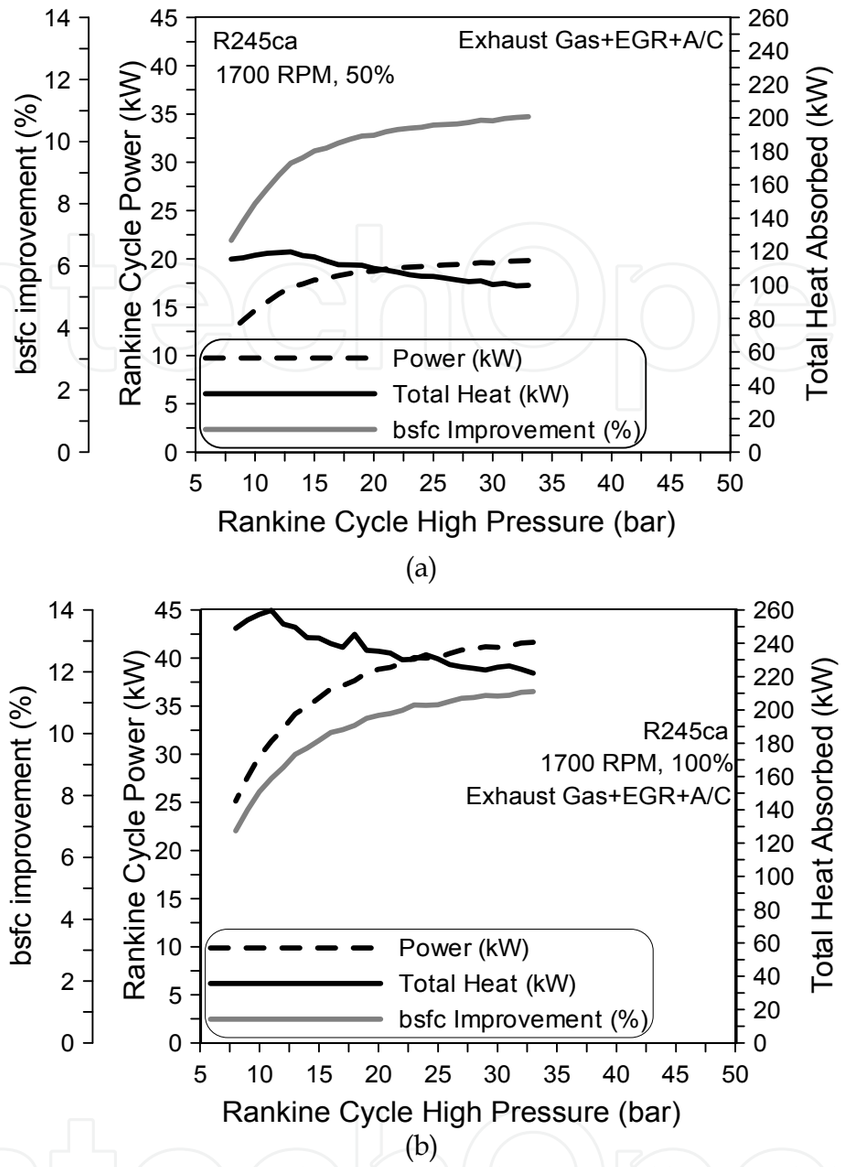

Fig. 16. bsfc improvement, generated powerand total recuperated heat absorbed by the organic (R245ca) Rankine cycle vs cycle high pressure, for 1700 rpm engine speed and three different loads of 50% (a) and 100% (b) with partially utilized EGR and CAC heat.

6. Benefits from the use of exhaust gas recuperation in HD diesel engines

Detailed investigations have been conducted to examine the effect of most promising technologies for exhaust heat recovery i.e., mechanical, electrical turbocompounding and Rankine cycle, on overall engine bsfc and power output. The results obtained from these detailed analyses have lead to the following conclusions:

- At a constant fuelling rate, both mechanical and electrical turbocompounding technologies result to reduction of primary engine power output. The effect on a percentage basis is higher at low engine load. However, both result to an improvement of overall power output due to the power generated from the waste exhaust gas.

- For mechanical turbocompounding, the optimum expansion ratio of the power turbine increases with engine load. But after a certain value in the range of 1.7-1.9 additional improvement is low considering the corresponding increase of exhaust pressure.
- As revealed from the analysis, mechanical turbocompounding can offer a maximum bsfc reduction of 0.5% at 25% load and 4.5% at full load for a power turbine efficiency of 80%. The overall bsfc benefit appears to be in the range of 2.5-3.4% at average engine load (75% engine load).
- Electrical turbocompounding can provide a maximum bsfc reduction of 6.5% using a highly efficient turbocharger. The improvement for a conventional T/C is smaller especially at low load. As revealed the maximum bsfc benefit is attributed by 2/3 to turbocompounding and 1/3 to the increase of T/C efficiency at full load. The situation is reversed at low load.
- Heat rejected from both the EGR cooler and CAC represents approximately 50% of the total heat rejected through the radiator of a heavy duty diesel. For this reason it should be considered the partial utilization of these heat amounts when attempting to reduce fuel consumption through heat recuperation. Apart from the obvious potential benefits in fuel consumption and power output the utilization of EGR cooler and CAC heat is promising for the reduction of the additional rejected heat from the Rankine cycle.
- As shown from the simulation results, a 20% increase in the case of steam and a 30% increase in the case of R245ca of radiator heat rejection capacity is adequate to successfully fulfill the additional demand for heat rejection of the diesel-Rankine power plant when both CAC and EGR heat is partially utilized. This is significantly lower compared to the case where EGR cooler and CAC heat is not utilized where the corresponding values are approximately double.
- For both steam and organic, when heat from both the EGR cooler and CAC is partially utilized the improvement in efficiency is almost 50% higher resulting to an equivalent increase of the excess generated power. This improvement is attributed more to the utilization of EGR cooler heat because it has a higher temperature allowing significant superheating of the steam.
- In the case of steam, the possibility to extend the high pressure (vaporization) in a much broader range allows better optimization of Rankine cycle operation compared to the organic.
- The maximum improvement in bsfc was observed in the case of the organic Rankine cycle and is ~ 11.3% when both EGR and CAC heat amounts are utilized. The corresponding value for steam is ~ 9%.
- The calculations reveal that recuperation of EGR and CAC heat improves system packaging significantly and that the dimensions of the additional radiator which also acts as a condenser for the Rankine cycle is almost the same with the existing diesel engine radiator.

7. Summary of results concerning exhaust gas recuperation in HD diesel engines

7.1 Expected overall efficiency gain from each technology

Considering the results presented in the previous sections as an outcome from detailed computational investigations, the potential bsfc reduction using the aforementioned exhaust heat recovery techniques is summarized in Table 4.

Technology	Current Realistic bsfc Reduction
Mechanical Turbocompounding	• **1**% at low engine load • **4.8**% at full engine load
Electrical Turbocmpounding	• **3.0-6.0**% for standard T/C efficiency • **6.0%-9.0**% with T/C efficiency of **65**%
Rankine With Steam	• bsfc reduction with steam is estimated at **6.0%-9.0**%.with an **expander efficiency of 70**% and max. high pressure value of **40** bar.
Rankine with Organic	• **9.0%-11.0**% expander efficiency of **70**% and max. high pressure value of 36 bar. • Potential improvement of bsfc with another working media.

Table 4. Potential bsfc Benefit of Various Technologies.

7.2 Benefits & drawbacks of each technological solution

Each of the aforementioned technologies presents various benefits and drawbacks. These are summarized in Table 5 below and should be considered for practical application.

Technology	Benefits	Disadvantages
Mechanical Turbocompounding	• Simplicity • Low volume & Cost.	• Interaction with engine • Relatively Low bsfc benefit. • Lower bsfc improvement at low load.
Electrical Turbocompounding	• Relative Simplicity • Low volume • Relatively good bsfc benefit	• Interaction with engine • Possible problem with electric power generation
Rankine With Steam	• Good bsfc reduction potential. • Low mass flow rate (negative impact on expander efficiency). • Small effect of engine load on bsfc benefit. • No interaction with engine.	• Complexity. • Volume and Weight. • Small expander efficiency with common technology. Microturbine technology can offer substantial improvement (Under investigation). • Possible fouling of heat exchanger without soot trap.
Rankine with Organic	• Highest bsfc reduction potential. • Small effect of engine load on bsfc benefit. • High mass flow rate (favorable for expander efficiency). • Lower heat exchanger area compared to steam.	• Complexity. • Volume and Weight. • Thermal and Chemical stability of organic fluid. • Toxicity considerations of working fluid. • Possible fouling of heat exchanger without soot trap.

Table 5. Benefits & Disadvantages of Exhaust Heat Recovery Techniques.

7.3 Most promising technologies for future investigation

Considering the results from the analysis and the advantages and disadvantages of the various technological solutions examined it is given in Table 6 their ranking with maximum of "*****".

Technology	bsfc benefit	Effect on Engine	Volume Weight	Cost	Applicability
Mechanical Turbocompounding	**	****	**	*	*****
Electrical Turbocompounding	***	***	**	**	****
Rankine With Steam	****	*****	*****	****	**
Rankine with Organic	*****	*****	****	*****	***

Table 6. Benefits & Disadvantages of Exhaust Heat Recovery Techniques.

8. Final conclusion

From the technological solutions considered, it results that each technology offers various benefits when considered for practical application. However we have to consider that the primary criterion in case of choice is in most cases, efficiency, i.e. "overall bsfc reduction".
Thus, the most promising technology appears to be Rankine Cycle with organic, followed by Rankine Cycle using Steam and finally Electric Turbocompounding.
Considering the first two solutions the problem appears to be complexity and size of required heat exchanger. The organic is favorable in this issue due to better thermodynamic characteristics. For steam, a problem exists resulting from its low mass flow rate which does not favor turbine efficiency. On the other hand this working media is favorable i.e water having no toxicity and easily replaceable (leakages). The aforementioned problem with steam could possibly be overcome using microturbine technology, which is currently under consideration. If this problem is solved and heat exchanger volume is reduced then Rankine Cycle with steam appears to be an attractive solution. On the other hand, electric turbocompounding offers relative simplicity but considerably lower bsfc reduction. The reduction in the size of exhaust gas heat exchanger when using Rankine cycle is highly favored by taking advantage of the (significant) heat amounts rejected in EGR cooler and CAC.
In conclusion, the most favorable technology appears to be Rankine Cycle with organic fluid. If the problem with expander efficiency using steam can be solved then Steam Rankine Cycle also becomes attractive. Electric turbocompounding should be considered if size and weight of previous components becomes a serious problem.

9. References

[1] Rakopoulos, C.D. and Hountalas, D.T., "Development and Validation of a 3-D Multi-Zone Combustion Model for the Prediction of a DI Diesel Engines Performance and Pollutants Emissions". SAE Transactions, Journal of Engines, Vol.107, pp.1413-1429, 1998.

[2] Hountalas, D.T., Mavropoulos, G.C., Zannis, T.C. and Schwarz, V. (2005a) Possibilities to achieve future emission limits for HD DI diesel engines using internal measures, SAE Paper No 2005-01-0377.

[3] Heywood, J.B., Internal Combustion Engine Fundamentals, McGraw-Hill, New York, 1988.

[4] Annand, W.J.D., "Heat Transfer in the Cylinders of Reciprocating Internal Combustion Engines", Proc. Inst. Mech. Engrs, 177, 973-990, 1963.

[5] Dent, J.C. and Derham, J.A., "Air Motion in a Four-Stroke Direct Injection Diesel Engine", Proc. Inst. Mech. Engrs, 188, 269-280, 1974.

[6] Ramos, J.I., Internal Combustion Engine Modeling, Hemisphere, New York, 1989.

[7] Jung, D and Assanis, D.N., "Multi-zone DI Diesel Spray Combustion Model for Cycle Simulation Studies of Engine Performance and Emissions", SAE Paper No 2001-01-1246.

[8] Borman, G.L. and Johnson, J.H., "Unsteady Vaporization Histories and Trajectories of Fuel Drops Injected into Swirling Air", SAE Paper No. 598C, National Powerplant Meeting, Philadelphia PA, 1962.

[9] Ueki, S. and Miura, A., "Effect of Difference of High Pressure Fuel Injection Systems on Exhaust Emissions from HD DI Diesel Engine", JSAE Review, 20, 555-561, 1999.

[10] Wickman, D.D., Senecal, P.K., Tanin, K.V., Reitz, R.D., Gebert, K., Barkhimer, R.L., Beck, N.J., "Methods and Results from the Development of a 2600 Bar Diesel Fuel Injection System", SAE Paper No 2000-01-0947.

[11] Tennant, D.W.H. and Walsham, B.E. (1989) "The turbocompound diesel engine", SAE Paper No. 89064.

[12] Wilson, D.E. (1986) The design of a low specific fuel consumption turbocompound engine, SAE Paper No.860072.

[13] Brands, M.C, Werner, J. and Hoehne, J.L. (1981) Vehicle Testing of Cummins Turbocompound Diesel Engine, SAE Paper No. 810073.

[14] Hountalas D.T., Katsanos C.O., Rogdakis E.D., Kouremenos D., Study of available exhaust gas heat recovery technologies for HD diesel engine applications, International Journal of Alternative Propulsion, 2006.

[15] Hopmann, U. (2004) "Diesel engine waste heat recovery utilizing electric turbocompound technology", Catterpillar, DEER Conference, San Diego, California, USA.

[16] Hopmann, U. and Algrain, M. (2003) "Diesel engine waste heat recovery utilizing electric turbocompound technology", Caterpillar Inc., Presentation in 2003 DEER Conference Newport Rhode Island.

[17] Teng H, Regner G, Cowland C. Waste heat recovery of heavy-duty diesel engines by organic Rankine cycle part I: hybrid power system of diesel and rankine engines. SAE paper no. 2007-01-0537; 2007.

[18] Teng H. Achieving high engine efficiency for heavy-duty diesel engines by waste heat recovery using supercritical organic-fluid Rankine cycle. SAE paper no. 2006-01-3522; 2006.

[19] Parimal PS, Doyle EF. Compounding the truck diesel engine with an organic Rankine cycle system. SAE paper no. 760343; 1976.

[20] Dibella FA, Di Nanno LR, Koplow MD. Laboratory and on-highway testing of diesel organic Rankine compound long-haul vehicle engine. SAE paper no. 830122; 1983.

[21] Doyle E, Di Nanno LR, Kramer S. Installation of a diesel-organic Rankine compound engine in a class 8 truck for a single-vehicle test. SAE paper no. 790646; 1979.

[22] Hideyo O, Shigeru O. Waste heat recovery of passenger car using a combination of Rankine bottoming cycle and evaporative engine cooling system. SAE paper no. 930880; 1993.

[23] Chen SK, Lin R. A review of engine advanced cycle and Rankine bottoming cycle and their loss evaluations. SAE paper no. 830124; 1983.

[24] Kadota M, Yamamoto K. Advanced transient simulation on hybrid vehicle using Rankine cycle system. SAE paper no. 2008-01-0310; 2008.

[25] Hounsham S, Stobart R, Cooke A, Childs P. Energy recovery systems for engines. SAE paper no. 2008-01-0309; 2008.

[26] Nelson C. Exhaust energy recovery. In: Proceedings of Directions in Energy-Efficiency and Emissions Research (DEER) conference, Dearborn, Michigan, August 3-6; 2009.

[27] Obieglo A, Ringler J, Seifert M, Hall W. Future efficient dynamics with heat recovery. In: Proceedings of Directions in Energy-Efficiency and Emissions Research (DEER) Conference, Dearborn, Michigan, August 3-6; 2009.

[28] Nelson C. Exhaust energy recovery. In: Proceedings of Diesel Engine-Efficiency and Emissions Research (DEER) Conference, Dearborn, Michigan, August 4-7; 2008.

[29] Kruiswyk RW. An engine system approach to exhaust waste heat recovery. In: Proceedings of Diesel Engine-Efficiency and Emissions Research (DEER) Conference, Dearborn, Michigan, August 4-7; 2008.

[30] Ringler J, Seifert M, Guyotot V, Huebner W. Rankine cycle for waste heat recovery of IC engines. SAE paper no. 2009-01-0174; 2009.

[31] Teng H. Improving fuel economy for HD diesel engines with WHR Rankine cycle driven by EGR cooler heat rejection. SAE paper no. 2009-01-2913; 2009.

[32] Charyulu DG, Singh G, Sharmac JK. Performance evaluation of a radiator in a diesel engine-a case study. Applied Thermal Engineering 1999;19:625-39.

[33] Lemmon EW, Huber ML, McLinden MO. NIST standard reference database 23: Reference Fluid Thermodynamic and Transport Properties-REFPROP. Version 8.0,

National Institute of Standards and Technology, Standard Reference Data Program, Gaithersburg, 2007.

[34] Bejan A, Kraus A. Heat transfer handbook. New Jersey: John Wiley & Sons; 2003.

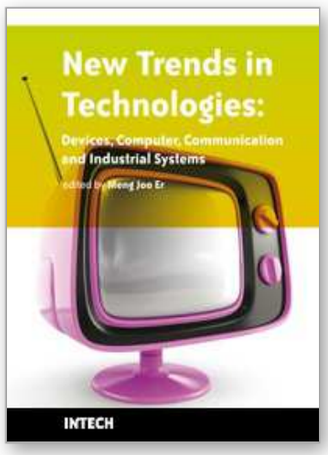

New Trends in Technologies: Devices, Computer, Communication and Industrial Systems
Edited by Meng Joo Er

ISBN 978-953-307-212-8
Hard cover, 444 pages
Publisher Sciyo
Published online 02, November, 2010
Published in print edition November, 2010

The grandest accomplishments of engineering took place in the twentieth century. The widespread development and distribution of electricity and clean water, automobiles and airplanes, radio and television, spacecraft and lasers, antibiotics and medical imaging, computers and the Internet are just some of the highlights from a century in which engineering revolutionized and improved virtually every aspect of human life. In this book, the authors provide a glimpse of new trends in technologies pertaining to devices, computers, communications and industrial systems.

How to reference
In order to correctly reference this scholarly work, feel free to copy and paste the following:

Dimitrios Hountalas and Georgios Mavropoulos (2010). Potential for Improving HD Diesel Truck Engine Fuel Consumption Using Exhaust Heat Recovery Techniques, New Trends in Technologies: Devices, Computer, Communication and Industrial Systems, Meng Joo Er (Ed.), ISBN: 978-953-307-212-8, InTech, Available from: http://www.intechopen.com/books/new-trends-in-technologies--devices--computer--communication-and-industrial-systems/potential-for-improving-hd-diesel-truck-engine-fuel-consumption-using-exhaust-heat-recovery-techniqu

INTECH
open science | open minds

InTech Europe
University Campus STeP Ri
Slavka Krautzeka 83/A
51000 Rijeka, Croatia
Phone: +385 (51) 770 447
Fax: +385 (51) 686 166
www.intechopen.com

InTech China
Unit 405, Office Block, Hotel Equatorial Shanghai
No.65, Yan An Road (West), Shanghai, 200040, China
中国上海市延安西路65号上海国际贵都大饭店办公楼405单元
Phone: +86-21-62489820
Fax: +86-21-62489821

IntechOpen